CEAS Aeronautical Journal
https://doi.org/10.1007/s13272-025-00900-8

ORIGINAL PAPER

Alternative fuels in aero engine performance calculations

Christian Klumpp[1] · Daniel Weintraub[2] · Sanket Girhe[3] · Stefan Henninger[1] · Heinz Pitsch[3] · Peter Jeschke[1]

Received: 31 March 2025 / Revised: 2 September 2025 / Accepted: 22 September 2025
© The Author(s) 2025

Abstract

This paper presents a method for gas turbine performance calculations with alternative fuels with a particular focus on their use in aircraft engines. The effects of various alternative aviation fuels on fuel consumption, CO_2 emissions, and contrail formation are examined in a comparative study. We use the GasTurb performance software and calculate heat release and hot section gas properties using a chemical equilibrium solver. Fuels with complex compositions are included in the calculation via surrogates of a limited number of known species that mimic the relevant properties of the real fuel. An automated method is used for the fuel surrogate formulation. We compare the results of this rigorous approach with the simplified approach of calculating the heat release using an alternative fuel's heating value while still using the gas properties of conventional Jet A-1. The results show that the latter approach systematically overpredicts fuel consumption by up to 0.2% for aromatics-free synthetic kerosene (e.g., "biofuels"). Overall, aircraft engines running on alternative fuels tend to be more fuel efficient due to their often higher hydrogen contents and thus fuel heating values. We find reductions in fuel consumption of up to 2.8% during cruise when using aromatics-free synthetic kerosene. We further assess how alternative fuels affect contrail formation based on the Schmidt-Appleman criterion. Contrails can form 200 m lower under cruise conditions when burning aromatics-free synthetic kerosene instead of Jet A-1 with identical thrust requirements and under the same atmospheric conditions, mainly due to their higher hydrogen content. In summary, we present a flexible yet easy-to-use method for studying fuel effects in performance calculations that avoids small but systematic errors by rigorously calculating the heat release and hot section gas properties for each fuel.

Keywords Alternative fuels · Sustainable aviation fuels (SAF) · Hydrogen · Performance · Aero engines · Gas turbines

List of symbol

Greek letters

γ	Specific heat ratio
ϵ	Ratio of molar masses of water and air, $\epsilon = M_{H_2O}/M_{air} = 0.622$
η_B	Burner efficiency
η_{ov}	Overall efficiency
ρ	Density
φ	Relative humidity
Ψ	Entropy function, Eq. (2)

Roman letters

c_{FHV}	Factor for *FHV*-correction, Eq. (11)
C_P	Heat capacity at P = const.
C_P^0	Molar heat capacity at P = const. for standard-state
EI_X	Emission index for species X
far	Fuel-to-air ratio (by mass)
F_N	Net thrust
FHV	Lower fuel heating value
G	Slope of the mixing line in a P_{H_2O} over T plot, Eq. (23)
h	Total specific enthalpy
H^0	Molar standard-state enthalpy
H/C	Ratio of hydrogen to carbon amount $\frac{n^H}{n^C}$
ΔH_{vap}	Enthalpy of vaporization
M	Molar mass
m	Mass fraction
n^X	Amount of species X
N_{Arom}	Number of aromatic species in the reactant
N_P	Number of target properties

✉ Christian Klumpp
klumpp@ist.rwth-aachen.de

[1] Institute of Jet Propulsion and Turbomachinery, RWTH Aachen University, Aachen, Germany

[2] GasTurb GmbH, Aachen, Germany

[3] Institute for Combustion Technology, RWTH Aachen University, Aachen, Germany

Published online: 14 October 2025

N_S	Number of product species
P	Total pressure
sfr	Steam-to-fuel ratio (by mass)
S^0	Molar standard-state entropy
T	Total temperature
V	Flight velocity
v_{Arom}	Aromatic content (by volume)
W	Mass flow rate
war	Water-to-air ratio (by mass)
wfr	Water-to-fuel ratio (by mass)
x	Mole fraction

Indices

amb	Ambient (static)
3	Engine station burner inlet
4	Engine station burner outlet
eq	Equilibrium state
F	Fuel
ref	Reference conditions
surr	Surrogate
tab	Fuel for which gas properties and heat release are tabulated

1 Introduction

Alternative aviation fuels derived from renewable sources are a promising technology for reducing the environmental impact of the aviation sector in the short and medium term future. They fall into two categories: Synthetic fuels that meet the specifications of *ASTM D7566* [1] can be blended with conventional Jet A-1 kerosene to be then referred to as drop-in fuels for use in aero-engines compliant with *ASTM D1655* [2], while all other fuels are referred to as non-drop-in fuels. A subset of these are near-drop-in fuels, which do not satisfy the standards but are close to doing so, e.g., synthetic kerosene that is too low in, or free of aromatics.

To compare different fuel candidates in engine performance calculations and to take into account fuel-related effects in preliminary design studies, heat release data and hot section gas properties for alternative fuels are required. In general, the assumption of constant or component-averaged gas properties is inadequate for quantitative gas turbine performance calculations, with errors reaching up to 5% and 1.5%, respectively [3]. This is due to their nonlinear dependence on temperature and gas composition in the hot section, where combustion products are present. Similarly, the assumption that heat release is proportional to the fuel-to-air ratio leads to errors of the same order of magnitude, because the increase in temperature rise of the combustion decreases significantly with increasing fuel-to-air ratios and the temperature rise reaches a maximum at stoichiometric conditions [4]. While both assumptions are often used in the context of teaching, state-of-the-art performance programs typically use pre-tabulated heat release and gas property data. The assumption of instantaneous attainment of chemical equilibrium is often used to calculate the values in these tables. This approach is sufficient for combustion modeling when only heat release is of interest, which is the case for performance calculations. More detailed modeling of the combustion processes would only be required if, for example, the formation of NO_X or soot emissions is of interest, which is not the focus of this paper. [5, 6]

Pre-tabulated data of heat release and gas properties can be created for example with the *NASA CEA (Chemical Equilibrium with Applications)* [7, 8] solver and are specific to each fuel [5, 9].

A simple approach to modeling alternative fuels, without the need to create new gas property and heat release tables, is to adjust the fuel heating value *FHV* to correct for the known heat release of a reference fuel such as conventional Jet A-1. We will refer to this approach as *FHV*-correction. This method still uses the gas properties of the reference fuel, which inherently introduces systematic errors, unlike the rigorous creation of fuel-specific gas property tables with a chemical equilibrium solver. For example, the *FHV* -correction overpredicts the fuel flow rate by up to 0.2% for aromatics-free, near-drop-in synthetic kerosenes and by more than 1% for hydrogen, as we show later in Sect. 4.1. The inaccuracies for (near-)drop-in fuels are small and may often be acceptable, especially for conceptual design studies, where many other sources of uncertainty must be considered. However, for applications that require higher accuracy and for non-drop-in fuels like hydrogen and methane, it is necessary to calculate the heat release and gas properties for the specific fuel in question. Litt and Chin [10] used the aforementioned NASA CEA solver to calculate these for two non-drop-in fuels, namely ethanol and ethyl stearate. Wolters et al. [11, 12] investigated synthetic kerosenes by approximating real fuels with one paraffinic and one aromatic species blended to match the aromatic content of several real fuels. This two-species fuel surrogate was then used to calculate the gas properties and heat release data with NASA CEA. Visser and Kluiters [13] developed a method for modeling alternative fuels within the *Gas Turbine Simulation Program (GSP)* [13, 14]. They introduced the option to specify a fuel either by the hydrogen-to-carbon H/C ratio and *FHV*, or by explicitly inputting the fuel composition. GSP performs the required chemical equilibrium calculations at runtime instead of using pre-tabulated values.

In summary, several authors have studied the effects of alternative fuels in the context of aircraft engine performance calculations, using methods ranging from the *FHV*-correction to the rigorous calculation of heat release and gas property data with a chemical equilibrium solver. The former leads to systematic errors as described above, and the latter requires

the availability of thermodynamic data functions fitted into so-called NASA polynomials [15]. These are only available for a few fuels besides conventional Jet A-1, such as methane, ethanol, or hydrogen. To extend this approach to other alternative fuels, it is necessary to formulate fuel surrogates consisting of species for which the thermodynamic data polynomials are known. The objective of this paper is to use, adapt, and combine established methods from the field of technical combustion, namely an automated formulation of fuel surrogates and a chemical equilibrium solver, to develop a flexible yet easy to use method to enable performance calculations for arbitrary alternative fuel candidates in conjunction with the GasTurb [16] performance software.

This paper is structured as follows: First, a brief introduction into the modeling of heat release and gas properties in engine performance calculations is given, followed by a detailed description of the two-step method developed in Sect. 3. Then, several methodological aspects are evaluated in Sect. 4, including a comparison between the developed rigorous method and the approximation with the *FHV* -correction. Finally, in Sect. 5, a selection of (near-)drop-in fuels is compared in terms of fuel consumption, emissions, and contrail formation for a state-of-the-art geared turbofan application.

2 Thermodynamic basics

This section gives a brief overview of the two fuel effects in performance calculations. These are the gas properties downstream of the combustor and the heat release in the combustor.

2.1 Gas properties

The effect of temperature and composition on gas properties, enthalpy, and entropy must be considered in quantitative performance calculations, as the use of constant gas properties introduces errors too large for any practical application, as discussed above. This is especially important in the hot section of a gas turbine where combustion products are present. The enthalpy function

$$h(T) = h_{T_{\mathrm{ref}}} + \int_{T_{\mathrm{ref}}}^{T} C_P(T)\mathrm{d}T \tag{1}$$

is often used to this end. For convenience, zero enthalpy is typically defined at $T_{\mathrm{ref}} = 298.15\,\mathrm{K}$ in the context of engine performance. In addition, the function

$$\Psi = \frac{1}{R}\int_{T_{\mathrm{ref}}}^{T} \frac{C_P(T)}{T}\mathrm{d}T \tag{2}$$

is used to calculate isentropic processes with

$$\Psi_2 = \Psi_1 + \ln\left(\frac{P_2}{P_1}\right). \tag{3}$$

Equation 2 is known as entropy function in the context of engine performance. As only differences in entropy function values are used, the reference values can be set arbitrarily and thus are not specified [4, 9].

In the GasTurb software, the gas properties, i.e., the specific heat ratio γ, the specific heat capacity C_P and the molar mass M, as well as the enthalpy and entropy functions are read from tables in the form

$$\gamma, C_P, M, h, \Psi = f(T, far, war). \tag{4}$$

The underlying gas model is half-ideal, i.e., the influence of temperature and composition is considered while that of pressure is neglected. The gas property tables as given by Eq. (4) are fuel-specific because the gas properties downstream of the combustor depend on the fuel composition, especially the hydrogen content of the fuel.

2.2 Heat release

In simplified calculations, for example in the context of teaching, the energy balance of the combustor is often simplified to

$$W_4 h_4 - W_3 h_3 \approx W_{\mathrm{F}} FHV \eta_{\mathrm{B}}, \tag{5}$$

where the enthalpy difference between the combustor exit and entry, stations 4 and 3, respectively, is calculated from the fuel flow rate W_{F}, the nominal fuel heating value *FHV* and the burner efficiency η_{B}. This simplification is not adequate for quantitative performance calculations as outlined above. The fuel heating value can be measured in the bomb calorimeter experiment as the heat released when the combustion products are cooled to the initial temperature T_{ref} in a constant volume [3, 17]. The reference conditions ($T_{\mathrm{air}} = T_{\mathrm{F}} = 288.15\,\mathrm{K}, P = 101.325\,\mathrm{kPa}$) for this experiment are very different from the conditions in a gas turbine combustor. In addition, dissociation must be taken into account at high combustion temperatures. We define the effective fuel heating value

$$FHV_{\mathrm{eff}} = \frac{W_4 h_4 - W_3 h_3}{\eta_{\mathrm{B}} W_{\mathrm{F}}} = f\left(T_3, P_3, far, T_{\mathrm{F}}\right) \tag{6}$$

to account for these effects throughout this paper.

The GasTurb software reads the combustion temperatures from fuel-specific tables in the form

$$T_4 = f\left(T_3, P_3, far, war, wfr, sfr\right), \tag{7}$$

where the composition is described by the fuel- and water-to-air ratio, *far* and *war*, respectively. In case of water or steam injection, the water- and steam-to-fuel ratios, *wfr* and

sfr, respectively, are used. We note that the effect of the fuel temperature T_F is neglected. We will evaluate the consequences of this simplification in Sect. 4.2. Incomplete combustion is accounted for with a burner efficiency η_B under 1. All operating points studied in this paper are at high thrust settings and therefore, we assume the burner efficiency to be constant at $\eta_B \approx 1$.

GasTurb calculates the fuel heating value from the tabulated heat release and gas property data, Eqs. (4) and (7), as

$$FHV_{tab} = \frac{(1+far)h_{Teq} - h_{T_{ref}}}{far}, \tag{8}$$

where T_{eq} refers to the equilibrium combustion temperature read from the heat release table and the enthalpy function is evaluated at

$$h_{T_{eq}} = h\left(T_{eq}\left(T_{ref}, P_{ref}, far_{ref}\right), far_{ref}\right) \tag{9}$$

and

$$h_{T_{ref}} = h\left(T_{ref}, far_{ref}\right). \tag{10}$$

For the *FHV* calculation, *war*, *wfr* and *sfr* are set to zero and are therefore omitted in the above equations. The reference conditions are $T_{ref} = 288.15\,\mathrm{K}$, $P_{ref} = 101.325\,\mathrm{kPa}$, and $far_{ref} = 0.02$, where the latter is a typical value for aero engines running on kerosene.

The fuel heating value calculated with Eq. (8) is also the basis for the *FHV*-correction that was already mentioned in the Introduction, Sect. 1, as a simplified approach for studying fuel effects in performance calculations. A simple correction is based on the ratio of the fuel heating values

$$c_{FHV} = \frac{FHV}{FHV_{tab}} \tag{11}$$

of the actual fuel and the fuel, for which the temperature rise data was tabulated. There are more sophisticated approaches, including calibration with fuel-specific factors, but these are not useful for studies of new fuels. During cycle calculations, the temperature rise is corrected by

$$T_4 = T_3 + c_{FHV}\left(T_{4,tab} - T_3\right), \tag{12}$$

where $T_{4,tab}$ refers to the combustion temperature of the fuel for which the table was created. We will analyze the errors from the *FHV*-correction later in Sect. 4.1.

2.3 Emission indices

CO_2 and H_2O are the main products of the combustion of any hydrocarbon fuel. Assuming complete combustion and neglecting the formation of other emissions such as CO or soot, the emission indices for CO_2 and H_2O can be calculated from the fuel composition alone. All carbon reacts with the available oxygen to CO_2 and EI_{CO_2} is only a function of the H/C-ratio and the molar masses

$$EI_{CO_2} = \frac{M_{CO_2} n_F^C}{M_F} = \frac{M_{CO_2}}{M_C + \mathrm{H/C}\, M_H}. \tag{13}$$

Analogously, the water emission index is calculated as

$$EI_{H_2O} = \frac{M_{H_2O}\, n_F^C\, \mathrm{H/C}}{2\, M_F} = \frac{\mathrm{H/C}\, M_{H_2O}}{2\left(M_C + \mathrm{H/C}\, M_H\right)}. \tag{14}$$

3 Method

To facilitate performance calculations with arbitrary fuels, two methods from the field of technical combustion are combined here: the calculation of the heat release and gas properties based on the assumption of chemical equilibrium and the automatic formulation of fuel surrogates for alternative fuels. The latter is required to be able to apply the chemical equilibrium solver to arbitrary fuels, the composition of which is often either unknown or too complex for practical calculations. Both methods and the combined workflow are described in this section.

3.1 Chemical equilibrium solver

In this paper, we calculate the chemical equilibrium according to the methods of Gordon and McBride [7, 8], which are also the basis of the widely used chemical equilibrium solver *NASA Chemical Equilibrium with Applications (CEA)*. The chemical equilibrium is found by minimizing the Gibbs free energy. Conservation of elements, mass, and energy are constraints on the minimization. An interactive web version of NASA CEA is available [18].

The gas properties are calculated as a $T, P = \text{const.}$ problem type. To get the simple table format of Eq. (4), where the gas composition is described only by *far* and *war*, only H_2O and CO_2 are considered as combustion products in addition to the other constituents of atmospheric air (N_2, O_2, Ar) for the gas property calculation [9].

The heat release is calculated as a $h, P = \text{const.}$ problem type and the resulting combustion temperatures are tabulated according to Eq. (7). In contrast to the calculation of the gas properties, pressure variations and all potential combustion products are taken into account. To simplify the calculations in this paper, only species with mole fractions greater than 10^{-6} are considered. For the combustion of Jet A-1, Kyprianidis et al. [5] identified these to be Ar, CO_2, H_2O, N_2, O_2, CO, H, HO_2, H_2, NO, NO_2, N_2O, O, and OH.

The inputs to the chemical equilibrium calculation are the composition of the oxidizers (air) and reactants (fuel), along with their respective temperatures, and the product species to be considered. It is necessary to provide thermodynamic data polynomials for the specific heat capacity $C_P^0(T)$, enthalpy $H^0(T)$, and entropy $S^0(T)$ for standard-state for all species. These polynomials are available for one representative kerosene fuel and several basic species in [15]. A more comprehensive collection is provided in [19]. However, thermodynamic data polynomials are not available for all alternative fuel candidates. To use the chemical equilibrium solver for them, we include a method for the automated formulation of fuel surrogates which is described in Sect. 3.2.

With the chemical equilibrium solver, the gas property and heat release tables defined by Eqs. (4) and (7), respectively, can be created. Both tables are stored in text files in the GasTurb property file format (.prp). Each property file is specific to a single fuel.

Conventional and (near-)drop-in aviation fuels are injected in their liquid form; however, the thermodynamic data polynomials for most species are only available in their gaseous form. To address this discrepancy, we have added a vaporization correction to the calculation of the initial enthalpy of the reactant according to

$$h_{0,F}(T) = \sum_{i=1}^{N_{S,F}} \begin{cases} n_i\left(H_i^0(T) - \Delta H_{\mathrm{vap},i}(T)\right) & \text{with vap. correction} \\ n_i H_i^0(T) & \text{no vap. correction} \end{cases}, \tag{15}$$

which requires the enthalpy of vaporization ΔH_{vap} to be known for each species of the fuel surrogate.

To allow for a seamless integration with the formulation of surrogates described in the next section as well as the GasTurb code, the relevant parts of the chemical equilibrium solver are implemented in Delphi following the description of the algorithm by Gordon and McBride [7]. A linear matrix solver from the *ALGLIB* package [20] is employed to solve the linear equation system encountered in the Gibbs free energy minimization.

To validate our implementation of the chemical equilibrium solver, we compare the results with those obtained using GasTurb Details [21] in conjunction with the original NASA CEA solver [8], which is the state-of-the-art code for such calculations. We use iso-octane, which is commonly used as a reference fuel [22] , as the reactant for this validation. Both the gas property and the heat release tables are in good agreement. The relative differences are less than 0.05% and 0.01% respectively. A closer analysis of the differences shows that most data points are in exact agreement, while for only a few data points much smaller numerical differences are amplified due to limited significant digits (five) in the NASA CEA output. Since thermodynamic data polynomials are available for liquid and gaseous iso-octane [15], we can also evaluate the vaporization correction, Eq. (15), by comparing the combustion temperatures calculated using the polynomials for gaseous iso-octane together with the vaporization correction to those calculated using the polynomials for liquid iso-octane. The results show that no additional uncertainties are introduced by the vaporization correction. In summary, the validation shows good agreement between the newly implemented equilibrium solver and NASA CEA. The vaporization correction is validated as well. For all subsequent studies, only gas property files generated with our new solver will be used.

3.2 Automated formulation of fuel surrogates

The calculation of gas properties and heat release with the chemical equilibrium solver described in the previous section requires thermodynamic property polynomials for all reactants as an input. While polynomials are available for generic kerosene and other basic fuels such as hydrogen or methane [15], a more generalized approach is required for arbitrary alternative fuels.

Real fuels, whether derived from petroleum or from alternative sources, consist of a large number of different species. In the field of technical combustion, it is standard practice to define fuel surrogates consisting of only a few species that mimic relevant fuel properties. Typically, kerosene surrogates consist of various n-, iso-, and cycloalkanes, as well as aromatics. This approach greatly reduces the complexity of numerical modeling and simulation. The composition of the fuel surrogate is chosen to accurately represent selected actual physical and chemical properties, for example, the hydrogen-to-carbon ratio H/C, the aromatic content v_{Arom}, or the fuel heating value *FHV* [22, 23]. It is important to note that the objective of this paper is to formulate fuel surrogates for heat release and gas property calculations with a chemical equilibrium solver only, thus matching properties relevant to emission modeling are not the focus here.

Several authors [24–26] have used the palette of recommended surrogate components proposed by Colket et al. [22] to automatically generate fuel surrogates by solving a constrained optimization problem. In this method, the surrogate components and target properties are prescribed, and the optimal mole fractions are determined numerically. Of course, the mole fraction x_i of each of the N_S species in the surrogate must be in the range

$$0 < x_i < 1 \text{ for } i = 1 \ldots N_S \tag{16}$$

while

$$\sum_{i=1}^{N_S} x_i = 1. \tag{17}$$

Various authors [24–26] developed the method mainly to create chemical kinetic models for numerical simulations. As target properties, they proposed the H/C-ratio to capture the heat release, the Cetane Number *CN* to capture the reactivity and the Threshold Sooting Index *TSI* to capture the sooting tendencies of the real fuel. For each of these properties, it is assumed that the property of the surrogate can be calculated from a weighted sum, by volume, mass, or mole fraction, of the corresponding property of each individual species.

In the context of performance calculations, the *FHV* is the most important fuel property because it determines the heat release and thus the fuel flow rate. The *FHV* of the surrogate can be calculated by the mass weighted sum

$$FHV_{\text{surr}} = \sum_{i=1}^{N_S} m_i FHV_i, \tag{18}$$

wherein FHV_i for each species is calculated with Eqs. (8) to (10). The calculation of the fuel surrogate's FHV_{surr} by the weighted sum approach is preferable to the calculation with Eqs. (8) to (10) because Eq. (18) can be included in a linear equation system. We compared the results of the weighted sum approach with the rigorous calculation and found the deviations to be much less than 0.01% for the (near-)drop-in fuels listed in Table 2.

In addition to the *FHV*, the H/C-ratio

$$(\text{H/C})_{\text{surr}} = \sum_{i=1}^{N_S} \frac{n_i^{\text{H}}}{n_i^{\text{C}}} \tag{19}$$

and the aromatic content

$$v_{\text{Arom}} = \frac{\sum_{i=1}^{N_{\text{Arom}}} x_i M_i / \rho_i}{\sum_{i=1}^{N_S} x_i M_i / \rho_i}, \tag{20}$$

are used as target properties in this paper to match the overall fuel composition. Both can be calculated directly from the surrogate composition and are commonly referenced in fuel specifications. If necessary, the surrogate formulation can be easily extended to include any additional properties that can be calculated from similar weighted sums.

The equations for the target properties (18) to (20) are rearranged to give the final problem statement as a linear equation system

$$A \cdot \vec{x} = \vec{b}, \tag{21}$$

where A is a $N_P \times N_S$ matrix, $\vec{x}$ is the result vector containing N_S mole fractions corresponding to the species considered in the surrogate and $\vec{b}$ is the right-hand side of N_P equations. Eqs. (16) and (17) are the constraints on $\vec{x}$. For the solution of the problem a least squares fitting function from the *ALGLIB* [20] package.

3.3 Performance calculations with alternative fuels

Two independent methods are presented above: the chemical equilibrium solver and the automated surrogate formulation. When combined as shown in Fig. 1, they enable performance calculations with alternative fuels.

The combined method uses a species database containing basic species such as H_2, O_2, CO_2, as well as a variety of additional species such as those proposed by Edwards et al. [22] as potential components for fuel surrogates. For each species, the chemical composition and thermodynamic data polynomials are enlisted in the database. For species that are potential components of fuel surrogates, additional properties such as density and heat of vaporization are supplemented.

The required inputs are a set of target properties (*FHV*, H/C, v_{Arom}), which may be taken from fuel specifications or published fuel analyses, and a selection of species for the surrogate formulation. With these inputs, the fuel surrogate is automatically formulated following the method described in Sect. 3.2. The properties of the species are read from the pre-assembled species database. The resulting fuel surrogate is the input for the next step, namely the creation of the property files containing gas property and heat release tables with the chemical equilibrium solver, as described in Sect. 3.1. Additional inputs required for this step are the composition of the oxidizer, which is typically atmospheric air, and some additional settings, such as minimum and maximum values and step sizes for each parameter in Eqs. (4) and (7). Again, all necessary properties of the species are read from the database. The result is a GasTurb property file (.prp) that can be used in the GasTurb software with any engine configuration and with all previously created engine models.

If the fuel composition is known or a mixture of known fuels, such as a hydrogen-methane mixture, is of interest, the surrogate formulation can be skipped. This is indicated by the second, dashed starting point in Fig. 1.

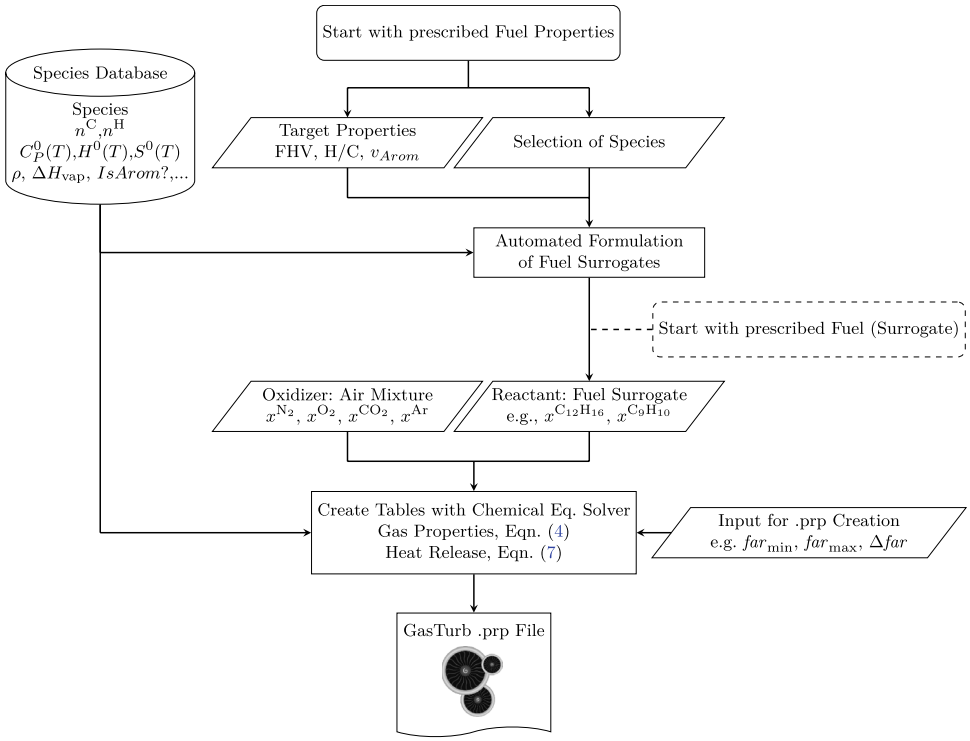

Fig. 1 Flowchart of the combined method to enable performance calculations with alternative fuels

4 Evaluation of methodological aspects

Before we continue with the comparison of different synthetic kerosenes, we want to highlight some methodological aspects in this section that may be of interest to engineers that are developing or using performance software.

4.1 Accuracy of the *FHV*-correction

In Sect. 2.2, the *FHV*-correction was introduced as a simplified method for considering the effects of alternative fuels on performance calculations. In this section, we will evaluate the accuracy of this correction by comparing the results with those obtained using fuel-specific gas property and heat release tables created with the method outlined above, which we also refer to as the rigorous calculation. The formulation of fuel surrogates used for this study is described later in Sect. 5.1, but the details are not relevant to the results presented in this section.

Two effects lead to inaccuracies when using the *FHV* -correction. First, the *FHV*-correction adjusts only the heat release, while the gas properties remain unchanged. Accordingly, for $far > 0$, a systematic error is introduced in the gas properties, if the combustion products differ from those of the fuel for which the tables were created, for example due to a higher hydrogen content of the fuel. Second, the *FHV*-correction itself is not exact, but only a linearized approximation of the complex combustion chemistry. To study both effects, we use a conventional fuel with a low *FHV* of 42.9 MJ/kg (C1, Table 2 in Sect. 5.1) as a reference. The alternative fuels studied are an aromatics-free synthetic kerosene with a high *FHV* of 44.1 MJ/kg (S3, Table 2 in Sect. 5.1) as well as hydrogen and methane as examples of non-drop-in fuels. The latter are included to push the errors to the extreme and to showcase the limitations of the *FHV* -correction.

Figure 2 shows the ratio of the specific heat capacity C_P of the combustion products of the alternative fuel to that of the conventional reference fuel $C_{P,\mathrm{ref}}$. The deviation is relatively constant with T but increases with far, as anticipated. Alternative fuels with higher H/C ratios lead to a higher water content in the combustion products, which results in their higher C_P compared to the combustion products of conventional kerosene. For the non-drop-in fuels methane and hydrogen, the errors in C_P when using the *FHV*-correction, i.e., using C_P of conventional kerosene, are significant, reaching up to 5% and 15%, respectively. For the near-drop-in synthetic kerosene, the errors are small, amounting to less than 0.05% in the relevant value range.

To evaluate the inaccuracies in the heat release calculation, we compare the effective fuel heating values, as given by Eq. (6). Figure 3 shows the ratio of the effective fuel heating value FHV_{eff} to that approximated with the *FHV*-correction $FHV_{\mathrm{eff,approx}}$. At reference conditions ($T_3 = 298.15$ K, $far = 0.02$), the error is zero as expected. For lower and higher values of T_3, the heat release is overpredicted when using the *FHV*-correction. This is because the correction factor c_{FHV} from Eq. (11) in Eq. (12) is not

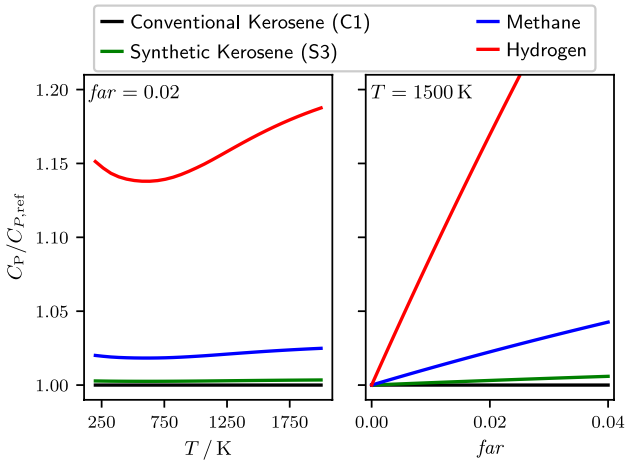

Fig. 2 Ratio of C_P of the combustion products of the alternative fuels to $C_{P,\mathrm{ref}}$ of the combustion products of the reference fuel (C1). Calculated with the method of Sect. 3.3. Fuel data for C1 and S3 are listed in Sect. 5.1, Table 2

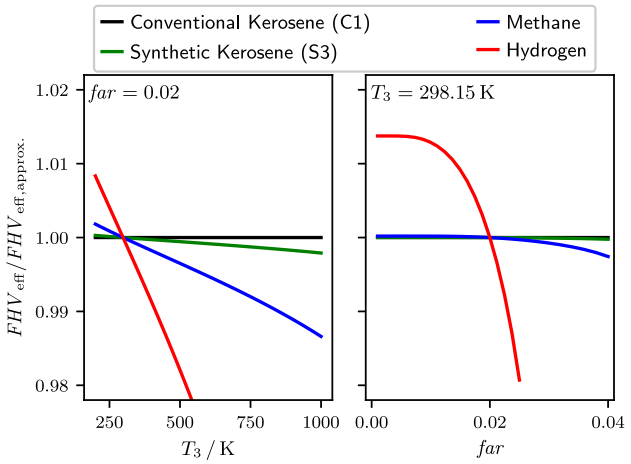

Fig. 3 Ratio of the effective fuel heating values FHV_{eff} calculated with the rigorous method of Sect. 3.3 to the approximated $FHV_{\mathrm{eff,approx}}$ calculated with the *FHV*-correction as given by Eqs. (11) and (12) with C1 as the tabulated reference fuel. Fuel data for C1 and S3 are listed in Sect. 5.1, Table 2

constant. An error is introduced by calculating c_{FHV} at reference conditions and applying it at all other inlet conditions. Since T_3 is typically much higher than 298.15 K in real engines, systematic errors in the fuel flow rate in performance calculations must be expected.

Next, we use the GasTurb software [16] to evaluate the influence of the two sources of error outlined above on a cycle calculation. As an example, we use a model of a two-spool geared turbofan with a sea-level static take-off thrust of 150 kN. The engine model is based on publicly available data, and all inputs are chosen to reflect current technology levels. Table 1 lists the fuel flow rate W_F and the burner exit temperature T_4 for both the rigorous calculation and the calculation using the *FHV*-correction.

It is apparent that with increasing *FHV* of the alternative fuels, and thus with increasing *FHV*-correction ratios as given by Eq. (11), the deviations in the calculated fuel flow increase. The errors for the near-drop-in synthetic kerosene are small (< 0.2%) and larger for methane and hydrogen, at 0.7% and 1.4%, respectively. In general, errors in the calculated fuel flow rate are much smaller than the *FHV* ratios in Fig. 3. This can be explained by partial error cancelation due to the opposite sign of the individual deviations in the specific heat capacities and the heat release. While the heat release is overpredicted (see Fig. 3), the heat capacity is underestimated (see Fig. 2) and thus the turbine power output is also lower. Additionally, the results show that the deviations in the thermodynamic quantities downstream of the burner, such as the burner exit temperature T_4, can be significant as shown, for example for hydrogen with an error of 101 K.

In summary, applying the *FHV*-correction to the non-drop-in fuels methane and hydrogen leads to significant errors, and therefore fuel-specific heat release and gas property tables should always be used. The inaccuracies for near-drop-in synthetic kerosene are small and may often be acceptable, especially for conceptual design studies, where many other sources of uncertainty must be considered. However, for applications that require higher accuracy, the method outlined in Sect. 3.3 eliminates these systematic errors.

Table 1 Comparison of cycle results at a take-off operating point (sea level static, $F_N = 150$ kN) using rigorously calculated fuel-specific heat release and gas property tables to those using the *FHV* -correction

Fuel	*FHV* (MJ/kg)	W_F (kg/s)			T_4 (K)		
		Rigorous	*FHV*-corr	Error	Rigorous	*FHV*-corr	Error
Conv. fuel (C1)	42.9	1.103	–	–	1721	–	–
Synthetic kerosene (S3)	44.1	1.073	1.074	+ 0.18%	1718	1724	+ 6 K
Methane	49.7	0.946	0.953	+ 0.74%	1701	1732	+31 K
Hydrogen	118.4	0.387	0.392	+ 1.40%	1674	1775	+ 101 K

The conventional fuel with the lowest *FHV* (C1) is used as reference fuel for the *FHV*-correction. Fuel data for C1 and S3 is listed in Table 2

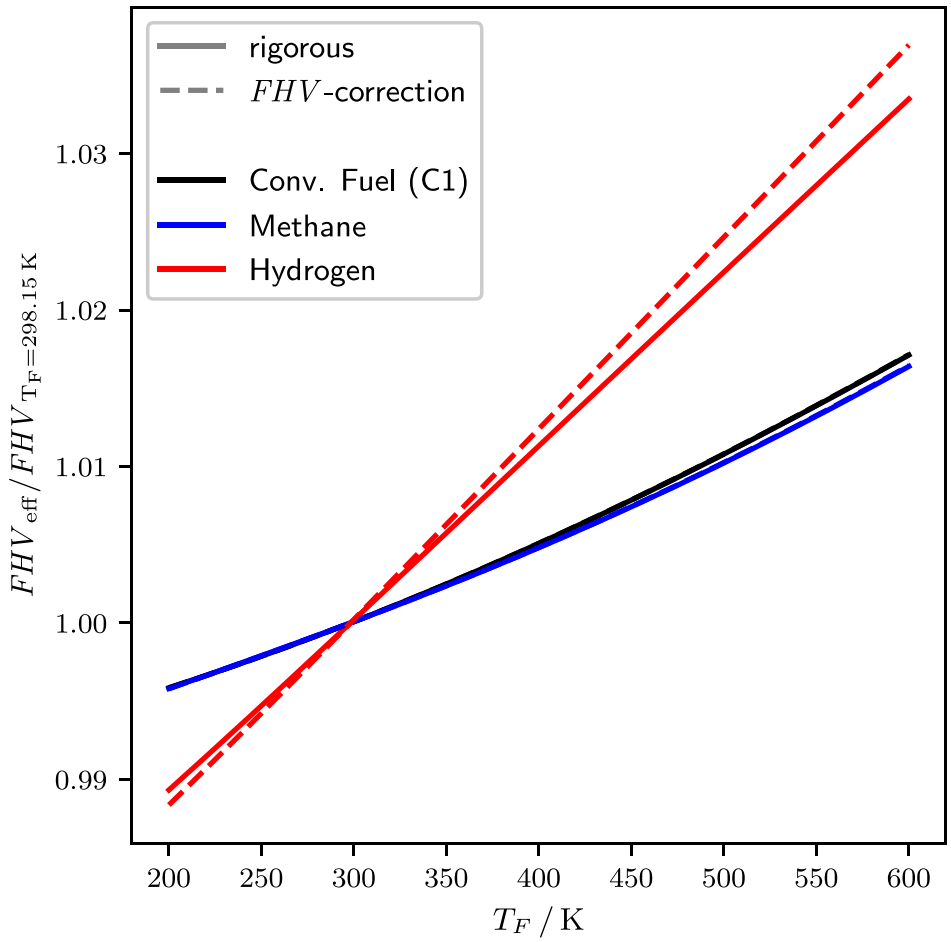

Fig. 4 Effective fuel heating value as a function of fuel temperature, relativized with $FHV_{T_{F=298.15\,K}}$. Calculated rigorously with Eq. (6) (solid lines) and approximated with the *FHV*-correction as given by Eqs. (12) and (22) (dashed lines). Fuel data for the conventional kerosene C1 is listed in Sect. 5.1, Table 2

Table 2 Reference fuel properties, properties of the final fuel surrogates and cycle results for fuel flow rate and CO_2-emissions for selected conventional (C1–C3) and synthetic (S1 to S6) kerosenes

Fuel	Reference fuel properties				Surrogate properties			Cycle results*	
	FHV (MJ/kg)	H/C	v_{Arom} (%)	References	*FHV* (MJ/kg)	H/C	v_{Arom} (%)	ΔW_F (%)	ΔW_{CO_2} (%)
C1	42.9	1.89	19.7	[27]	42.9	1.89	19.7	Ref	Ref
C2	43.0	1.92	17.2	[29]	43.0	1.92	17.2	− 0.22	− 0.44
C3	43.1	1.90	18.3	[28]	43.1	1.90	18.4	− 0.43	− 0.51
S1	43.8	2.15	0.5	[28]	43.8	2.15	0.5	− 2.11	− 3.92
S2	44.1	2.15	0.0	[29]	44.0	2.16	0.1	− 2.72	− 4.52
S3	44.1	2.17	0.4	[29]	44.1	2.17	0.4	− 2.79	− 4.72
S4	43.5	2.06	9.3	[27]	43.5	2.06	9.3	− 1.51	− 2.71
S5	43.5	2.04	11.3	[27]	43.5	2.04	11.3	− 1.34	− 2.40
S6	43.2	1.92	17.0	[28]	43.2	1.93	17.1	− 0.69	− 0.90

*Cruise operating point (F_N = 23 kN in 10,668 m with Mach 0.78), see Sect. 5.2

4.2 Fuel temperature effect

The fuel temperature T_F has an influence on the heat release as mentioned in Sect. 2.2. The heat release tables used by the GasTurb software are in the form of Eq. (7), which means that the temperature effect is neglected. Therefore, they are strictly valid only for one fuel temperature, which by default is T_F = 298.15 K.

It is possible to include an approximate correction without adding a dimension to the heat release tables using the *FHV*-correction as given by Eq. (12) with the correction factor

$$c_{FHV} = 1 + \frac{h_F(T_F) - h_F(T_{F,ref})}{FHV_{T_{F,ref}}}, \quad (22)$$

where $FHV_{T_{F,ref}}$ refers to the fuel heating value calculated with the reference fuel temperature $T_{F,ref}$ for which the heat release table was created.

Figure 4 shows the effect of the fuel temperature on the effective fuel heating value FHV_{eff} for three fuels: Conventional kerosene (C1, Table 2 in Sect. 5.1), methane and hydrogen. Two lines are plotted for each fuel: The solid lines are rigorously calculated using the fuel temperature as an input to Eq. (6) and the dashed lines are approximated using Eqs. (12) and (22). The effect of the fuel temperature is most pronounced for hydrogen, which has a much higher specific heat capacity. For hydrogen, FHV_{eff} varies between −1% and +3% compared to the reference FHV at $T_{F,ref} = 298.15$ K over the plotted temperature range of 200 K to 600 K. This is especially relevant, because many past and present research projects are investigating the potential of using hydrogen as a heat sink before injecting it as a fuel in aero engines and thus its fuel temperature can vary significantly. The comparison of the two calculation methods in Fig. 4 shows that the errors introduced using the FHV-correction instead of the rigorous calculation are at most 0.3% at $T_F = 600$ K for hydrogen. The errors are below 0.1% for conventional kerosene and methane.

4.3 Interpolation errors due to the use of tabulated gas property and heat release data

Many performance programs use tabulated heat release and gas property data for improved speed and robustness compared to using a chemical equilibrium solver nested within the performance code. However, there are inherent drawbacks to this approach. First, simplifications such as the omission of the fuel temperature discussed above are necessary to reduce the dimensions of the tabulated data. Second, systematic errors result from the interpolations required when reading from tabulated data. As an example, this section gives an overview of the expected magnitude of interpolation errors based on the interpolation methods and step sizes used by default by the GasTurb software. It is important to note that the errors listed below are worst case scenarios where interpolation is required at the midpoint between two support points. For most calculations, much smaller inaccuracies can be expected. All results below are calculated with the chemical equilibrium solver described in Sect. 3.1 with a fuel surrogate for conventional kerosene (C1, Table 2 in Sect. 5.1).

To evaluate the heat release, the combustion temperature T_4 is read from tables in the form of Eq. (7). Values for T_3 are tabulated by default in steps of $\Delta T_3 = 200$ K and quadratic interpolation is used. The maximum interpolation error for T_4 between two values of T_3 is ±0.5 K. The errors practically vanish with a reduction to a step size of $\Delta T_3 = 50$ K. The interpolation errors in T_4 over P_3, which is tabulated on a logarithmic scale for four values of P_3, are up to −1 K at $T_3 = 1000$ K for $far < 0.04$. The errors of the linear interpolation of T_4 over far are under −1.5 K for $far < 0.04$ with the default step size of $\Delta far = 0.005$.

The gas properties are tabulated in the form of Eq. (4) for two fuel-to-air ratios, pure air ($far = 0$) and for the highest far at which the temperature rise increases during combustion, which for kerosene is in the range $far = 0.06$ to 0.07. The resulting errors of the linear interpolation of C_P between the two far values are on the order of ±0.18% while the errors of the linear interpolation over T are below ±0.1% with the default step size of $\Delta T = 100$ K. Halving the step sizes significantly reduces the interpolation errors to below ±0.03%.

In summary, the use of tabulated heat release and gas property data in performance calculations inherently introduces interpolation errors that are reasonably small when appropriate step sizes and interpolation methods are used. If higher accuracy is desired, the interpolation errors can be easily reduced by using smaller step sizes, without the need to use a nested chemical equilibrium solver within the performance code.

5 Results

5.1 Formulation of fuel surrogates

In this section we formulate fuel surrogates for drop-in and near-drop-in aviation fuels using the method described in Sect. 3.2. The fuel surrogates are formulated by solving a system of linear equations, where the unknown compositions of preselected surrogate components are determined to match the chosen properties of the surrogate with those of the real fuel. A least squares minimization with constraints is used to solve the system of linear equations and thus there is usually no unique, exact solution, even when the number of equations, i.e., the number of target properties, is equal to the number of independent variables, i.e., the number of surrogate components. In this study, we evaluate different combinations of target properties, such as FHV, H/C, and ν_{Arom}, and surrogate components in terms of their ability to accurately reproduce the relevant properties of the real fuel. Most importantly, the FHV of the fuel surrogates must match the FHV of the real fuel with an error of less than 0.1%. Otherwise, the small differences in heating value of less than 3% between the (near-)drop-in fuel candidates from Table 2 cannot be captured.

The fuel properties are listed in Table 2. The fuels have been tested in aero engines by research groups who have reported the results of detailed fuel analyses [27–29]. The synthetic aviation fuels can be classified as near-drop-in fuels. The fuels are divided into three groups, conventional kerosenes that meets Jet A-1 or JP-8 specifications (C1 to C3), one fuel produced by *Fischer-Tropsch* synthesis (S1), and synthetic kerosenes from biomass (S2 to S6). Of the latter, S2 to S5 are synthesized by the *Hydroprocessed Esters and Fatty Acids (HEFA)* process, and S6 is synthesized by *Catalytic Hydrothermolysis*.

First, we characterize the fuels only by their aromatic content, i.e., we use v_{Arom} as the only target property for the surrogate formulation. We include three surrogate components, n-decane, methylcyclohexane, and m-xylene. This selection is adopted from Pepiot and Narayanaswamy et al. [24, 25] with one modification: replacing n-dodecane with n-decane. We do this because the H/C-ratio of n-decane is higher, which is crucial when creating surrogates for alternative fuels with H/C-ratios that exceed that of n-dodecane (H/C > 2.167), which is typical for fuels with little or no aromatic content. The *FHV* of the resulting fuel surrogates differ from the reference values by ±1%, which is almost as large as the *FHV* variation between the fuels themselves and much larger than our target deviation of less than 0.1%. Therefore, we find that characterizing fuels by their aromatic contents alone is not sufficient for performance calculations.

Next, we use the same surrogate components but add the H/C ratio as a second target property in addition to the aromatic content. This change halves the deviations of the *FHV* to ±0.5%, which is still larger than the requirement. We conclude that *FHV* must be used explicitly as a target property to accurately formulate fuel surrogates for performance calculations.

Finally, we use all three properties (*FHV*, H/C, v_{Arom}) as targets for the surrogate formulation and increase the number of surrogate components to find a surrogate that reproduces all three target properties for all fuels from Table 2. We find that this is the case when seven species are included in the surrogate formulation. Tables 2 and 3 list the properties and composition of the fuel surrogates, respectively. We want to point out that we do not propose these surrogates for general use, but only use them in heat release and gas property calculations with a chemical equilibrium solver for our performance calculations in Sects. 4, 5.2 and 5.3. The results of this section apply to the limited selection of fuels from Table 2 and the surrogate components studied here.

5.2 Impact of alternative fuels on engine performance and emissions

In this section we analyze the effect of the (near-)drop-in fuels from Table 2 on fuel consumption and CO_2 emissions. We use the GasTurb software with gas property and heat release tables created for each fuel as described in Sect. 3.3 with fuel surrogates formulated as described above. For all studies, we use a two-spool geared turbofan engine with a sea-level static take-off thrust of 150 kN. The engine model is based on publicly available data, and all inputs are chosen to reflect current technology levels. All fuels are (near-)drop-in fuels that, if certified, are ready for use in today's fleet. Accordingly, the engine design remains unchanged and all calculations are performed in the off-design mode.

Table 2 lists the reduction in fuel consumption and CO_2 emissions compared to the conventional kerosene with the lowest *FHV* (C1) for a cruise operating point at 10,668 m with Mach 0.78 and a thrust of $F_N = 23$ kN.

The conventional fuels with higher *FHV* reduce the fuel flow rate by up to 0.4% for C3. The reduction for the aromatics-free fuels with high H/C ratios is significantly higher, reaching up to 2.8% for the synthetic kerosene with the highest *FHV* (S3).

Table 3 Composition of seven component fuel surrogates. *FHV*, H/C, and v_{Arom} were used as target properties in the automated surrogate formulation as described in Sect. 3.2

	Mole fractions (%)						
	n-, iso-, and cyclo-paraffins						Aromatic
Identifier	n-decane	n-tetradecane	Iso-octane	Iso-dodecane	Methylcyclo-hexane	Decalin	m-xylene
C1	9.6	3.5	15.5	8.9	26.9	10.8	24.9
C2	8.5	1.7	15.8	12.7	33.5	6.2	21.7
C3	0	52.0	0	0	0	18.0	30.0
S1	8.1	5.2	28.5	37.4	19.1	1.0	0.77
S2	91.3	0	0	0	0	8.5	0.2
S3	68.6	30.6	0	0	0	0	0.7
S4	14.8	0.6	36.4	13.6	21.0	1.1	12.5
S5	4.0	1.0	38.2	27.4	10.8	2.6	16
S6	0	57.8	0	0	0	13.5	28.7

The fuel data is listed in Table 2

With respect to CO_2 emissions, the reduction reaches up to 4.7% for the (near-)drop-in fuels. This is due to the combined effect of the lower fuel consumption and the lower carbon content, which according to Eq. (13) results in a lower EI_{CO_2}. It is important to note that these values refer only to the CO_2 emissions of the combustion and not those of the entire life cycle, which are ideally zero for sustainable aviation fuels.

5.3 Impact of alternative fuels on contrail formation

The contrail formation is affected by the type of fuel used. This can be demonstrated using the Schmidt-Appleman criterion, which goes back to the work of Schmidt [30] and Appleman [31]. A detailed discussion is also provided by Schumann [32]. We calculate the slope of the mixing line of engine exhaust and ambient air as

$$G = \frac{EI_{H_2O}\, C_P\, p_{amb}}{\epsilon\, FHV\left(1-\eta_{ov}\right)}, \tag{23}$$

following Schumann [32]. The water emission index EI_{H_2O} depends on the fuel composition and is calculated as given by Eq. (14), ϵ is a constant and refers to the molar mass ratio of water and air, and the overall efficiency of the engine is defined as

$$\eta_{ov} = \frac{F_N V}{W_F\, FHV}, \tag{24}$$

where F_N is the net thrust and V is the flight velocity. If the mixing line intersects the saturation curve for water, the Schmidt-Appleman criterion is satisfied and contrails can form. Figure 5 shows the mixing lines for conventional kerosene (C1), one synthetic kerosene (S3), hydrogen, and methane. A truly fair comparison with the latter non-drop-in fuels would require a redesign of the engine. However, for the purpose of demonstrating the order of magnitude of their influence on contrail formation, we assume for this study that they function as drop-in fuels without any modifications to the engine or cycle.

To better demonstrate the impact of alternative fuels on contrail formation, we did not use the cruise operating point from Sect. 5.2 for this plot, but an operating point at an altitude of 9100 m. This is because at cruise altitude (10, 668 m), the Schmidt-Appleman criterion is satisfied for all fuels, whereas Fig. 5 now shows a case where the Schmidt-Appleman criterion is satisfied for the alternative fuels but not for the conventional kerosene. This is due to the higher H/C and consequently EI_{H_2O}, see Eq. (14), of the alternative fuels.

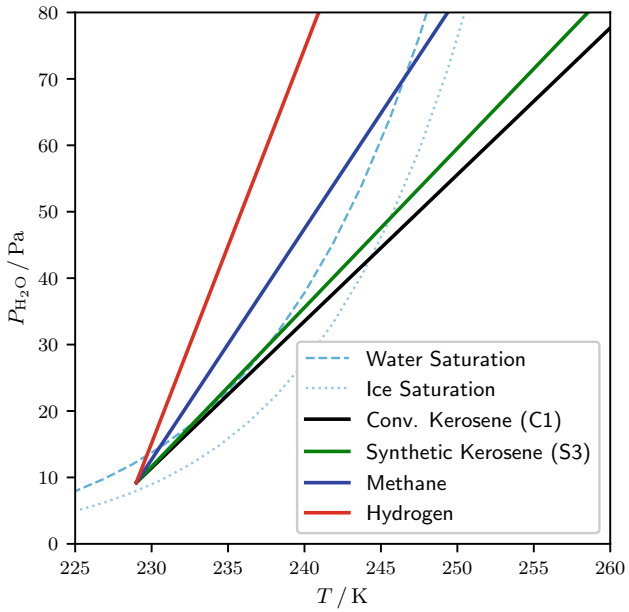

Fig. 5 Mixing lines of engine exhaust and ambient air for different fuels in a water partial pressure versus temperature plot at a cruise operating point (9100 m, $M = 0.78$, $\varphi = 75\%$, $F_N = 23$ kN)

Assuming a constant thrust requirement at all altitudes and ISA standard atmospheric conditions, we can convert this result to an altitude difference of 200 m between the onset of contrails for the synthetic kerosene and conventional kerosene. This difference increases to 1 km for methane and more than 2 km for hydrogen. These numbers are to be taken as preliminary estimates, given these large altitude differences, the change in thrust requirements at different altitudes should be taken into account. However, the general trends and magnitudes are very clear. Additionally, we want to emphasize that these results are obtained based on a simplified analysis using the Schmidt-Appleman criterion. Other effects on contrail formation, such as the influence of gaseous and particulate emissions, were out of the scope of this study.

This indicates that alternative fuels cause contrails already at lower altitudes, which could somewhat counter their otherwise positive effect on aviation's climate impact. To put this into context, we want to note that the ability to form contrails in itself does not indicate whether they are persistent or have a significant climate impact. Despite the formation of contrails in slightly lower altitudes, alternative fuels can still provide a significant benefit in terms of climate impact, see e.g., [33].

6 Conclusion

We have presented above a method for rigorous analysis of fuel effects in gas turbine performance calculations that uses a chemical equilibrium solver to calculate hot section gas properties and heat release in conjunction with an automated formulation of fuel surrogates. In this way, accurate performance calculations can be carried out for any alternative fuel, no matter how complex in composition, as long as three key properties (*FHV*, H/C ratio, v_{Arom}) are known. We have implemented the chemical equilibrium solver and automated fuel surrogate formulation and linked it to the GasTurb performance software.

We demonstrate that systematic errors introduced by the *FHV*-correction, which approximates fuel effects by adjusting only the heat release and not the hot section gas properties, are eliminated with our method. For a state-of-the-art geared turbofan at take-off operating conditions, the *FHV*-correction leads to an overprediction of the fuel flow rate of up to 0.2% for (near-)drop-in fuels and more than 1% for non-drop-in fuels such as hydrogen. The burner exit temperature T_4 is overpredicted by more than 5 K and 100 K, respectively. It is evident that accurate performance calculations with non-drop-in fuels require fuel-specific gas property and heat release data. For (near-)drop-in fuels, the errors resulting from the *FHV*-correction are small and may be acceptable in many cases, especially in conceptual design studies where many additional sources of uncertainty must be considered. However, for applications where higher accuracy is desired, we recommend a method such as the one presented in this paper to eliminate a source of systematic error.

We further show that the influence of fuel temperature on heat release is relevant when the fuel temperature exceeds the reference temperature of $T_{\mathrm{F}} = 298.15\,\mathrm{K}$, especially for hydrogen which has 3% higher heat release at $T_{\mathrm{F}} = 600\,\mathrm{K}$ due to its higher specific heat capacity compared to kerosene, which has only a 1% higher heat release at $T_{\mathrm{F}} = 600\,\mathrm{K}$. For rigorous calculations, fuel temperature must be included as an additional dimension in the tabulated heat release data. Alternatively, if a maximum error of 0.3% is acceptable, the influence of fuel temperature can be corrected for using the *FHV*-correction approach.

Finally, a comparison of different alternative fuel candidates shows that a 2.8% reduction in cruise fuel consumption is possible with (near-)drop-in fuels, which can be realized with the current fleet and infrastructure, subject to fuel certification and availability. However, due to the higher hydrogen content of most alternative fuels, the Schmidt–Appleman criterion predicts contrail formation at about 200 m lower altitudes.

We recommend using methods such as those presented in this paper for pre-design and performance calculations involving alternative fuels, in particular when high accuracy is required. To facilitate this, the methods will be integrated into a future version of the GasTurb software.

Acknowledgements This research received funding as part of the AKaTri project, a research project supported by the Federal Ministry for Economic Affairs and Climate Action in the German Aviation Research Program.

Author Contributions C.K. prepared the main manuscript, developed the method and conducted the studies. D.W. supported the development of the method from a performance perspective and provided valuable feedback for improving the manuscript. S.G. supported the development of the method from a combustion perspective. All authors reviewed the manuscript and provided numerous comments for improvement.

Funding Open Access funding enabled and organized by Projekt DEAL.

Data Availability No datasets were generated or analyzed during the current study.

Declarations

Conflict of interest The authors declare no Conflict of interest.

Open Access This article is licensed under a Creative Commons Attribution 4.0 International License, which permits use, sharing, adaptation, distribution and reproduction in any medium or format, as long as you give appropriate credit to the original author(s) and the source, provide a link to the Creative Commons licence, and indicate if changes were made. The images or other third party material in this article are included in the article's Creative Commons licence, unless indicated otherwise in a credit line to the material. If material is not included in the article's Creative Commons licence and your intended use is not permitted by statutory regulation or exceeds the permitted use, you will need to obtain permission directly from the copyright holder. To view a copy of this licence, visit http://creativecommons.org/licenses/by/4.0/.

References

1. ASTM: ASTM D7566-23b: Specification for Aviation Turbine Fuel Containing Synthesized Hydrocarbons (2024). http://www.astm.org/cgi-bin/resolver.cgi?D7566-23B. Accessed 2 Sept 2025
2. ASTM: ASTM D1655-24b: Standard Specification for Aviation Turbine Fuels (2024). http://www.astm.org/cgi-bin/resolver.cgi?D1655-24B. Accessed 2 Sept 2025
3. Walsh, P.P., Fletcher, P.: Gas Turbine Performance, 2nd edn. Wiley (2004)
4. Kurzke, J.A.: Simplifications in gas turbine performance calculations. Paper presented at the ASME Turbo Expo 2007, Montreal, Canada, 2007 (1978)
5. Kyprianidis, K.G., et al.: Uncertainty in gas turbine thermo-fluid modelling and its impact on performance calculations and emissions predictions at aircraft system level. Proc. Inst. Mech. Eng. Part G J. Aerospace Eng. **226**, 163–181 (2012). https://doi.org/10.1177/0954410011406664
6. Hammond, D.C., Mellor, A.M.: Analytical calculations for the performance and pollutant emissions of gas turbine combustors. Combust. Sci. Technol. **4**, 101–112 (1971)

7. Gordon, S., McBride, B.J.: Computer Program for Calculation of Complex Chemical Equilibrium Compositions and Applications. Part 1: Analysis. Technical Report, NASA (1994). https://ntrs.nasa.gov/citations/19960044559
8. Gordon, S., McBride, B.J.: Computer Program for Calculation of Complex Chemical Equilibrium Compositions and Applications. Part II: Users Manual and Program Description. Technical Report, NASA (1996). https://ntrs.nasa.gov/citations/19960044559
9. Kurzke, J., Halliwell, I.: Propulsion and Power, 2nd edn. Springer, Cham (2025). https://doi.org/10.1007/978-3-031-65026-0
10. Litt, J.S., Chin, J.C., Liu, Y., Engineering, R., Heights, P.: Simulating the Use of Alternative Fuels in a Turbofan Engine. Technical Report, TM2013-216547, NASA (2013). https://ntrs.nasa.gov/citations/20140000928
11. Wolters, F.: Impact of alternative fuels on engine performance and CO2-emissions (2012). https://www.icas.org/icas_archive/ICAS2012/papers/737.pdf. Paper presented at the 28th International Congress of the Aeronautical Sciences, Brisbane, Australia (2012)
12. Wolters, F.: Einfluss alternativer drop-in Flugturbinenkraftstoffe auf das Emissionsverhalten des globalen Luftverkehrs. Ph.D. thesis, Ruhr-Universität Bochum (2020). https://elib.dlr.de/137470/
13. Visser, W.P., Kluiters, S.C.A.: Modelling the effects of operating conditions and alternative fuels on gas turbine performance and emissions. NLR-TP-98629, NLR (1998). https://reports.nlr.nl/bitstream/10921/1240/1/TP-1998-629.pdf. National Aerospace Laboratory NLR
14. Kluiters, S.C.A., Visser, W.P.J., Rademaker, E.R.: A new combustor and emission model for the gas turbine simulation program GSP. Technical Report, Memorandum VH-98-010, National Aerospace Laboratory, 1998, Amsterdam (2014). https://gspteam.com/Files/Publications/NLR-TR-2014-150.pdf
15. McBride, B.J., Zehe, M.J., Gordon, S.: NASA Glenn Coefficients for Calculating Thermodynamic Properties of Individual Species. Technical Report, NASA (2002). https://ntrs.nasa.gov/citations/20020085330
16. GasTurb GmbH: GasTurb 14: Gas Turbine Performance Software (2022). www.gasturb.com
17. ASTM: ASTM D4809: Standard Test Method for Heat of Combustion of Liquid Hydrocarbon Fuels by Bomb Calorimeter (Precision Method) (2024). http://www.astm.org/cgi-bin/resolver.cgi?D7566-23B. Accessed 2 Sept 2025
18. Gordon, S., McBride, B.J.: CEARUN rev4. https://cearun.grc.nasa.gov/. Accessed 2 Sept 2025
19. Burcat, A., Ruscic, B.: Third millenium ideal gas and condensed phase thermochemical database for combustion (with update from active thermochemical tables). Technical Report ANL-05/20, Argonne National Lab. (ANL), Argonne, IL (United States) (2005). https://www.osti.gov/biblio/925269
20. Bochkanov, S.: ALGLIB. https://www.alglib.net. Accessed 2 Sept 2025
21. GasTurb Details 6: An Utility for GasTurb (2021)
22. Colket, M., et al.: Development of an Experimental Database and Kinetic Models for Surrogate Jet Fuels. Paper presented at the 45th AIAA Aerospace Sciences Meeting and Exhibit, Reno, Nevada (2007)
23. Dagaut, P., Cathonnet, M.: The ignition, oxidation, and combustion of kerosene: a review of experimental and kinetic modeling. Progress Energy Combust. Sci. **32**, 48–92 (2006)
24. Pepiot, P.: Automatic strategies to model transportation fuel surrogates. Ph.D. thesis (2008). https://pepiot.mae.cornell.edu/pdf/Pepiot_Thesis.pdf
25. Narayanaswamy, K., Pitsch, H., Pepiot, P.: A component library framework for deriving kinetic mechanisms for multi-component fuel surrogates: application for jet fuel surrogates. Combust. Flame **165**, 288–309 (2016). https://doi.org/10.1016/j.combustflame.2015.12.013
26. Yu, J., Wang, Z., Zhuo, X., Wang, W., Gou, X.: Surrogate definition and chemical kinetic modeling for two different jet aviation fuels. Energy Fuels **30**, 1375–1382 (2016). https://doi.org/10.1021/acs.energyfuels.5b02414. (**Publisher: American Chemical Society**)
27. Sundararaj, R.H., et al.: Combustion and emission characteristics from biojet fuel blends in a gas turbine combustor. Energy **182**, 689–705 (2019). https://doi.org/10.1016/j.energy.2019.06.060
28. Chan, T.W., Chishty, W.A., Canteenwalla, P., Buote, D., Davison, C.R.: Characterization of emissions from the use of alternative aviation fuels. J. Eng. Gas Turbines Power **138**, 011506 (2016). https://doi.org/10.1115/1.4031226. (**Publisher: American Society of Mechanical Engineers**)
29. Klingshirn, C.D., et al.: Hydroprocessed renewable jet fuel evaluation, performance, and emissions in a t63 turbine engine. J. Eng. Gas Turbines Power **134**, 051506 (2012). https://doi.org/10.1115/1.4004841
30. Schmidt, E:. Die Entstehung von Eisnebel aus den Auspuffgasen von Flugmotoren (1941). https://elib.dlr.de/107948/ 44(44), 1–15. Verlag R. Oldenbourg, München Volume: 5
31. Appleman, H.: The formation of exhaust condensation trails by jet aircraft. Bull. Am. Meteorol. Soc. **34**, 14–20 (1953)
32. Schumann, U.: On Conditions for Contrail Formation from Aircraft Exhausts. Meteorol. Z. **5**, 4–23 (1996)
33. Teoh, R., et al.: Targeted use of sustainable aviation fuel to maximize climate benefits. Environ. Sci. Technol. **56**, 17246–17255 (2022). https://doi.org/10.1021/acs.est.2c05781. (**Publisher: American Chemical Society**)

Publisher's Note Springer Nature remains neutral with regard to jurisdictional claims in published maps and institutional affiliations.